

# Atomic Structure of a Cesium Aluminosilicate Geopolymer: A Pair Distribution Function Study

Jonathan L. Bell,<sup>†</sup> Pankaj Sarin,<sup>†</sup> John L. Provis,<sup>‡</sup> Ryan P. Haggerty,<sup>†</sup>  
Patrick E. Driemeyer,<sup>†</sup> Peter J. Chupas,<sup>§</sup> Jannie S. J. van Deventer,<sup>‡</sup> and  
Waltraud M. Kriven<sup>\*†</sup>

Department of Materials Science and Engineering, University of Illinois at Urbana–Champaign, Urbana, Illinois 61801, X-ray Science Division, Advanced Photon Source, Argonne National Laboratory, Argonne, Illinois 60439, and Department of Chemical and Biomolecular Engineering, University of Melbourne, Victoria 3010, Australia

Received November 27, 2007. Revised Manuscript Received March 14, 2008

The atomic pair distribution function (PDF) method was used to study the structure of cesium aluminosilicate geopolymer ( $\text{Cs}_2\text{O} \cdot \text{Al}_2\text{O}_3 \cdot 4\text{SiO}_2 \cdot x\text{H}_2\text{O}$ , with  $x \sim 11$ ). The geopolymer was prepared by reacting metakaolin with cesium silicate solution followed by curing at 50 °C for 24 h in a sealed container. Heating of Cs-geopolymer above 1000 °C resulted in formation of crystalline pollucite ( $\text{CsAlSi}_2\text{O}_6$ ). PDF refinement of the pollucite phase formed displayed an excellent fit over the 10–30 Å range when compared with a cubic pollucite model. A poorer fit was attained from 1–10 Å due to an additional amorphous phase present in the heated geopolymer. On the basis of PDF analysis, unheated Cs-geopolymer displayed structural ordering similar to pollucite up to a length scale of  $\sim 9$  Å, despite some differences. Our results suggest that hydrated  $\text{Cs}^+$  ions were an integral part of the Cs-geopolymer structure and that most of the water present was not associated with Al–OH or Si–OH bonds.

## Introduction

With the increasing worldwide availability of synchrotron sources and computing capabilities, the X-ray pair distribution function (PDF) method has become a formidable tool in the analysis of complex or disordered materials over the past several years.<sup>1–3</sup> By utilizing the full range of information accessible from a powder diffraction experiment, that is, diffuse as well as Bragg scattering, valuable insight can be gained into short- to medium-range order in amorphous or nanocrystalline materials, such as disordered zeolites,<sup>4,5</sup> poorly crystalline nanocomposites,<sup>6</sup> gels,<sup>7</sup> and glasses.<sup>8</sup> For these materials, structural details are typically inaccessible by more conventional diffraction methods due to the absence of Bragg peaks.

The PDF,  $G(r)$ , is defined as the Fourier sine transform of the reduced structure function  $F(Q) = Q[S(Q) - 1]$ , according to eq 1:<sup>2</sup>

$$G(r) = \frac{2}{\pi} \int_0^\infty Q[S(Q) - 1] \sin(Qr) dQ \quad (1)$$

Here  $Q = (4\pi \sin \theta)/\lambda$ , with  $\theta$  being the scattering angle and  $\lambda$  the wavelength of the incident radiation. The structure factor  $S(Q)$  is calculated from experimental scattering data (X-ray scattering in this case, although the use of neutrons is also popular) according to eq 2:<sup>1</sup>

$$S(Q) = \frac{I_{\text{el,coh}}(Q) + [\langle f(Q) \rangle^2 - \langle f(Q)^2 \rangle]}{\langle f(Q) \rangle^2} \quad (2)$$

$I_{\text{el,coh}}(Q)$  is the observed elastic and quasi-elastic coherent scattering intensity, “ $\langle \rangle$ ” represents a compositional average, and  $f(Q)$  is the atomic scattering amplitude. Calculation of  $I_{\text{el,coh}}(Q)$  from X-ray scattering data requires corrections for experimental factors such as sample holder and background and X-ray polarization, as well as other scattering events, in particular Compton scattering.

It is also possible to calculate a theoretical  $G(r)$  from a known structure using eq 3, thereby enabling real-space Rietveld refinement by comparison of the calculated and experimental PDFs:<sup>9</sup>

$$G_{\text{calc}}(r) = -4\pi r \rho_0 + \frac{1}{r} \sum_{ij} \frac{b_i b_j}{\langle b \rangle^2} \delta(r - r_{ij}) \quad (3)$$

In this equation,  $\rho_0$  is the average number density of the sample,  $b$  is the atomic form factor for X-rays, and the sum is carried out over all atom pairs  $i, j$ .

**Geopolymers.** Geopolymers are a class of alkali aluminosilicate materials which are gaining increasing attention

\* Corresponding author. E-mail: kriven@illinois.edu.

<sup>†</sup> University of Illinois at Urbana–Champaign.

<sup>‡</sup> University of Melbourne.

<sup>§</sup> Argonne National Laboratory.

(1) Egami, T. *Mater. Trans. JIM* **1990**, *31*, 163.

(2) Egami, T.; Billinge, S. J. L. *Underneath the Bragg Peaks: Structural Analysis of Complex Materials*; Pergamon: Amsterdam, 2003.

(3) Proffen, T.; Billinge, S. J. L.; Egami, T.; Louca, D. Z. *Kristallogr.* **2003**, *218*, 132.

(4) Martinez-Inesta, M. M.; Lobo, R. F. *J. Phys. Chem. B* **2005**, *109*, 9389.

(5) Martinez-Inesta, M. M.; Peral, I.; Proffen, T.; Lobo, R. F. *Microporous Mesoporous Mater.* **2005**, *77*, 55.

(6) Petkov, V.; Parvanov, V.; Trikalitis, P.; Malliakas, C.; Vogt, T.; Kanatzidis, M. G. *J. Am. Chem. Soc.* **2005**, *127*, 8805.

(7) Schmücker, M.; Schneider, H. J. *Sol-Gel. Sci. Technol.* **1999**, *15*, 191.

(8) Petkov, V.; Billinge, S. J. L.; Shastri, S. D.; Himmel, B. *Phys. Rev. Lett.* **2000**, *85*, 3436.

(9) Proffen, T.; Billinge, S. J. L. *J. Appl. Crystallogr.* **1999**, *32*, 572.

as potential refractory materials and as a low CO<sub>2</sub> producing alternative to cement. They comprise a gel binder phase and often contain unreacted inclusions.<sup>10</sup> Some geopolymers, specifically those with Si/Al ratios close to 1.0, have been shown to contain crystalline zeolites embedded within their gel structure.<sup>11–13</sup> Geopolymers with higher Si/Al ratios (e.g., Si/Al = 2) are widely understood to be X-ray amorphous, although it has been suggested that ordering may exist at atomic length scales.<sup>14,15</sup> However, literature is particularly lacking in the understanding of the atomic structure of geopolymers. Most of the insight gained into the geopolymer structure so far has been from nuclear magnetic resonance investigations and is restricted only up to the next nearest neighbors. The PDF method, particularly using X-ray scattering data collected at synchrotron sources, holds considerable promise in elucidating geopolymer structures extending up to 30 Å. A recent PDF study<sup>13</sup> of metakaolin-based geopolymers was limited in real space resolution, thus complicating analysis of local and intermediate structures.

Geopolymers are generally synthesized using group I K<sup>+</sup> or Na<sup>+</sup> as the charge-balancing alkali cation, leaving Cs-based geopolymers relatively unexplored, although some attention has been paid to these compositions for treatment of radioactive waste streams.<sup>16</sup> Heating of Cs<sub>2</sub>O·Al<sub>2</sub>O<sub>3</sub>·4SiO<sub>2</sub>·*m*H<sub>2</sub>O (*m* ≈ 7–13) geopolymers results in formation of crystalline pollucite (CsAlSi<sub>2</sub>O<sub>6</sub>).<sup>17</sup> Pollucite, a zeolitic phase, is a naturally occurring mineral and is of significant industrial interest as an encapsulant for radioactive <sup>137</sup>Cs,<sup>18–20</sup> as well as a refractory material, due to its high melting point and very low coefficient of thermal expansion.<sup>21</sup> In this study, the thermal transformation of a Cs-geopolymer precursor to crystalline pollucite was systematically investigated with the primary aim of understanding the structure of as-synthesized geopolymer.

## Experimental Section

Cesium silicate solution was made by dissolving cesium hydroxide hydrate (CsOH·*x*H<sub>2</sub>O, with *x* ~ 15–20%, 99.9% metals

Table 1. Samples Analysis Using the PDF Method

sample ID	heat treatment <sup>a</sup>	composition
CsGP	unheated	CsAlSi <sub>2</sub> O <sub>6</sub> ·11H <sub>2</sub> O
CsGP0900-00	900 °C, no soak	CsAlSi <sub>2</sub> O <sub>6</sub>
CsGP1000-00	1000 °C, no soak	CsAlSi <sub>2</sub> O <sub>6</sub>
CsGP1050-00	1050 °C, no soak	CsAlSi <sub>2</sub> O <sub>6</sub>
CsGP1100-00	1100 °C, no soak	CsAlSi <sub>2</sub> O <sub>6</sub>
CsGP1150-00	1150 °C, no soak	CsAlSi <sub>2</sub> O <sub>6</sub>
CsGP1200-00	1200 °C, no soak	CsAlSi <sub>2</sub> O <sub>6</sub>
CsGP1250-00	1250 °C, no soak	CsAlSi <sub>2</sub> O <sub>6</sub>
CsGP1100-24	1100 °C, 24 h soak	CsAlSi <sub>2</sub> O <sub>6</sub>
MK	unheated	2SiO <sub>2</sub> ·Al <sub>2</sub> O <sub>3</sub>
MK0900-00	900 °C, no soak	2SiO <sub>2</sub> ·Al <sub>2</sub> O <sub>3</sub>
CsOH	unheated	10.1 M CsOH

<sup>a</sup> All samples were heated and cooled at 10 °C/min to the specified set point.

basis, Alfa Aesar, Ward Hill, MA) in deionized water, followed by addition of a proportional amount of amorphous fumed silica (Cabot EH-5, T. H. Hilson Company, Wheaton, IL) such that the Cs:Si:H<sub>2</sub>O in solution was 1:1:5.5 on a molar basis. All calculations were made using *x* = 20% in the formula CsOH·*x*H<sub>2</sub>O for the commercial cesium hydroxide hydrate. The extra 0.2 mol of water was accounted for in the preparation of the cesium silicate solution. The solution was allowed to equilibrate for 1 week prior to addition of metakaolin for geopolymer synthesis. Geopolymer of composition CsAlSi<sub>2</sub>O<sub>6</sub>·5.5H<sub>2</sub>O (Cs<sub>2</sub>O·Al<sub>2</sub>O<sub>3</sub>·4SiO<sub>2</sub>·11H<sub>2</sub>O) was then prepared by mixing the cesium silicate solution with metakaolin (Engelhard HRM, Iselin, NJ). The resultant slurry was cast into 50 mL polypropylene tubes, sealed, and allowed to cure and set at 50 °C for 24 h. The cylindrical shaped, hardened geopolymer samples were then removed from the tubes and were ground using an alumina mortar and pestle and sieved through a 200 mesh (75 μm) standard sieve. The coarse particles >75 μm in size were discarded and only fine particles were used for further studies.

Differential scanning calorimetry (DSC) and thermal gravimetric analysis (TGA) studies were conducted on Cs-geopolymer powder (sample CsGP in Table 1) using a Netzsch STA409 CD instrument. Sample powders (~20–30 mg) were mounted in an alumina pan and were heated to 1300 °C at 10 °C/min under a gas flow that was comprised of He (25 mL/min) and air (50 mL/min). Careful examination of the sample holders after the experiment confirmed that there was no reaction between the sample powder and the alumina pans during these studies. In addition, equal amounts of CsGP sample powder were separately heat treated in an electrical furnace to various temperatures, up to 1250 °C. Details of sample heating conditions are listed in Table 1. Each powder sample was subsequently characterized for both elemental and crystalline phase composition by energy dispersive spectroscopy (EDS) and X-ray diffraction (XRD), respectively. A laboratory-based Rigaku (D-Max II) X-ray powder diffractometer (Rigaku/USA Inc., Danvers, MA), equipped with a Cu Kα source (*λ* = 0.1540598 nm) and a single crystal monochromator in the diffracted beam path, was used to acquire XRD patterns in Bragg–Brentano geometry over a 2θ range of 5–75° with a step size of 0.02°. Elemental composition studies were conducted on specimens that were prepared by mechanically pressing the powder samples into small, disc-shaped pellets. A minimum of six EDS spectra were collected from different regions of pressed disk samples using a JEOL 6060 LV SEM at 20 KeV and 1000× magnification for each sample. Copper was used as a calibration standard for the EDS measurements.

The sample heated to 1100 °C for 24 h was also characterized for crystalline phase composition using synchrotron X-rays at the Advanced Proton Source (Sector 33BM-C, UNICAT beam line at Argonne National Laboratory, Argonne, IL). The powder sample was mounted in a 0.3 mm glass capillary (Charles Supper Company,

- (10) Steveson, M.; Sagoe-Crentsil, K. *J. Mater. Sci.* **2005**, *40*, 2023.
- (11) Palomo, A.; Glasser, F. P. *Br. Ceram. Trans. J.* **1992**, *91*, 107.
- (12) Provis, J. L.; Lukey, G. C.; van Deventer, J. S. J. *Chem. Mater.* **2005**, *17*, 3075.
- (13) Rowles, M. The Structural Nature of Aluminosilicate Inorganic Polymers: A Macro to Nanoscale Study. Ph.D. Thesis, Department of Applied Physics, Curtin University of Technology, Perth, Australia, 2004.
- (14) Duxson, P.; Provis, J. L.; Lukey, G. C.; Mallicoat, S. W.; Kriven, W. M.; van Deventer, J. S. J. *Colloids Surf., A* **2005**, *269*, 47.
- (15) Provis, J. L.; Duxson, P.; Lukey, G. C.; van Deventer, J. S. J. *Chem. Mater.* **2005**, *17*, 2976.
- (16) Blackford, M. G.; Hanna, J. V.; Pike, K. J.; Vance, E. R.; Perera, D. S. *J. Am. Ceram. Soc.* **2007**, *90*, 1193.
- (17) Kriven, W. M.; Bell, J. L.; Mallicoat, S. W.; Gordon, M. Intrinsic Microstructure and Properties of Metakaolin-Based Geopolymers. *International Workshop on Geopolymer Binders—Interdependence of Composition, Structure and Properties*; Bauhaus-Universität Weimar: Weimar, Germany, 2006; p 71.
- (18) Gallagher, S. A.; McCarthy, G. J. *J. Inorg. Nucl. Chem.* **1981**, *43*, 1773.
- (19) Hess, N. J.; Espinosa, F. J.; Conradson, S. D.; Weber, W. J. *J. Nucl. Mater.* **2000**, *281*, 22.
- (20) Xu, H. W.; Navrotsky, A.; Balmer, M. L.; Su, Y. L. *J. Am. Ceram. Soc.* **2002**, *85*, 1235.
- (21) Beall, G. H.; Rittler, H. L. *Adv. Ceram. Nucl. Cryst. Glasses* **1982**, *4*, 301.

Natick, MA) and rotated at 60 rpm. A curved image plate (CIP) detector apparatus, described elsewhere,<sup>22</sup> was used to collect high resolution X-ray diffraction data at 22.5 keV ( $\lambda \approx 0.5515 \text{ \AA}$ ) over a  $2\theta$  range of  $0\text{--}37^\circ$  in transmission geometry with a step size of  $0.00095^\circ$ . The wavelength and image plate setup were calibrated using the LaB<sub>6</sub> standard (NIST SRM 660a, National Institute of Standards and Technology, Gaithersburg, MD). Rietveld refinements were carried out using Jade 7 software (Minerals Data Inc., Livermore, CA).

Total scattering studies were conducted on Cs-geopolymer samples at the Argonne National Laboratory at the Advanced Photon Source, beam line 11ID-B ( $\sim 90.3 \text{ keV}$ ,  $\lambda = 0.1372 \text{ \AA}$ ). The use of high energy not only minimizes the unwanted effects of sample absorption and multiple scattering but also enables the collection of data at high wave vectors.<sup>23</sup> Powder samples were mounted in polyimide tubes (of outer diameter 2.84 mm; Accellent Cardiology, Trenton, GA), and X-ray scattering data was collected in transmission geometry. An amorphous silicon detector (General Electric Revolution Radiography Detector) was used to collect high resolution X-ray scattering data for  $Q \geq 30 \text{ \AA}^{-1}$ , although  $Q_{\text{max}} = 27 \text{ \AA}^{-1}$  was used as a cutoff value during the PDF analysis. This image plate detector is capable of rapid acquisition ( $\sim 7.5$  frames/sec) having a high spatial resolution ( $2048 \times 2048$  pixels, with each pixel being  $200 \times 200 \text{ }\mu\text{m}$ ) as described by Chupas et al.<sup>24</sup> The sample to detector distance (calculated as 229.158 mm), detector tilt, angle of rotation, and zero position were determined using the CeO<sub>2</sub> standard (SRM 674a, NIST, Gaithersburg, MD). Besides the geopolymer samples, additional samples such as (a) 10.1 M CsOH solution, (b) unheated metakaolin, and (c) metakaolin heated to  $900^\circ\text{C}$  were also analyzed by the PDF method (see Table 1).

The contribution of light elements to Compton scattering at high  $Q$  and high energy is often greater than the elastic signal<sup>2</sup> and may not be accurately accounted for when using tabulated values. It is therefore important to ensure good scattering statistics and a high signal-to-noise ratio. For the geopolymer samples, 100–200 frames were collected at 6–10 s/frame, resulting in an overall exposure time which ranged from 10 to 33 min. In an earlier study using this detector, 7 min of exposure time was found to be adequate to yield acceptable statistics up to  $Q_{\text{max}} = 35 \text{ \AA}^{-1}$ , for amorphous SiO<sub>2</sub> samples.<sup>24</sup>

Further processing of X-ray scattering data sets was done using the software program Fit2D and included summation of all the frames collected for each sample, correction for polarization and geometrical effects, and conversion to a one-dimensional scattering data set as a function of  $Q$ .<sup>25,26</sup> This data set was further corrected for sample holder and background scattering, image plate geometry, and Compton scattering using the program PDFgetX2 to generate a normalized and corrected total scattering function,  $Q[S(Q) - 1]$ .<sup>27</sup> Absorption and multiple scattering corrections were not required as they were found to be negligible under the high energy and transmission geometry setup used.<sup>24</sup> The Fourier sine transform of the corrected and normalized data then yielded the reduced PDF

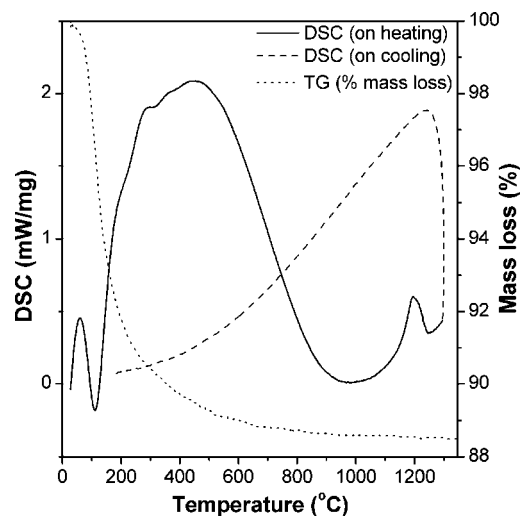


**Figure 1.** DSC and TGA for CsGP at a heating rate of  $10^\circ\text{C/min}$ . An exotherm representative of cubic pollucite crystallization reached a maximum at  $1196^\circ\text{C}$ .

function,  $G(r)$ , according to eq 1. Calculated PDFs for the geopolymer samples were compared to a cubic pollucite model using the program PDFFIT.<sup>9</sup>

## Results and Discussion

**Transformation of Cs-Geopolymer to Pollucite.** Heating of  $\text{Cs}_2\text{O} \cdot \text{Al}_2\text{O}_3 \cdot 4\text{SiO}_2 \cdot 11\text{H}_2\text{O}$  geopolymer resulted in the formation of crystalline pollucite ( $\text{CsAlSi}_2\text{O}_6$ ). Thermal analysis studies confirmed that upon heating, CsGP first undergoes drying which is characterized by weight loss and is followed by crystallization into pollucite. Simultaneous DSC and TGA results are shown in Figure 1 for CsGP heated to  $1300^\circ\text{C}$  at  $10^\circ\text{C/min}$ . Overall, approximately 12% weight loss was observed during the DSC/TGA studies and was attributable mainly to loss of water. It should be noted that this weight loss was in addition to any loss of water when the cast Cs-geopolymer sample was ground into fine powder or while it was stored before the DSC/TGA studies. In geopolymers, water is present in micro- and nanosized pores as free water, on the free surfaces as adsorbed water, and also as chemically bound  $-\text{OH}$  groups.<sup>28</sup> The endothermic peak observed at  $110^\circ\text{C}$  corresponds to evaporation of free water from the pores in the geopolymer structure. The majority of the free and adsorbed water loss occurs below  $250^\circ\text{C}$  and is followed by condensation of  $-\text{OH}$  groups at higher temperatures.<sup>29</sup> The broad exothermic peak in the DSC curve at  $\sim 1196^\circ\text{C}$  is due to crystallization of CsGP into pollucite, as confirmed by XRD, shown in Figure 2.

The XRD pattern of unheated geopolymer displayed a number of broad diffuse peaks which coincided with those of crystalline pollucite phase formed on heating above  $1000^\circ\text{C}$  (Figure 2). This is in contrast with the XRD patterns of sodium or potassium geopolymer having a  $\text{Si/Al} \geq 2$ , which usually has a single broad diffuse peak near  $2\theta$  of  $30^\circ$  (for  $\text{Cu K}\alpha$  radiation).<sup>30</sup> Samples heated to higher temperatures

(22) Sarin, P.; Haggerty, R. P.; Yoon, W.; Kriven, W. M.; Knapp, M.; Zschack, P. *Ceram. Eng. Sci. Proc.* **2006**, *27*, 313.

(23) Petkov, V.; Qadir, D.; Shastri, S. D. *Solid State Commun.* **2004**, *129*, 239.

(24) Chupas, P. J.; Chapman, K. W.; Lee, P. L. *J. Appl. Crystallogr.* **2007**, *40*, 463.

(25) Hammersley, A. P. *Fit2D: An Introduction and Overview*; ESRF Internal Report, ESRF97HA02T; European Synchrotron Radiation Facility: Grenoble, France, 1997.

(26) Hammersley, A. P.; Svensson, S. O.; Hanfland, M.; Fitch, A. N.; Hausermann, D. *High Pressure Res.* **1996**, *14*, 235.

(27) Qiu, X.; Thompson, J. W.; Billinge, S. J. L. *J. Appl. Crystallogr.* **2004**, *37*, 678.

(28) Rahier, H.; VanMele, B.; Wastiels, J. *J. Mater. Sci.* **1996**, *31*, 80.

(29) Duxson, P.; Lukey, G. C.; van Deventer, J. S. J. *J. Mater. Sci.* **2007**, *42*, 3044.

(30) Davidovits, J. J. *Therm. Anal.* **1991**, *37*, 1633.



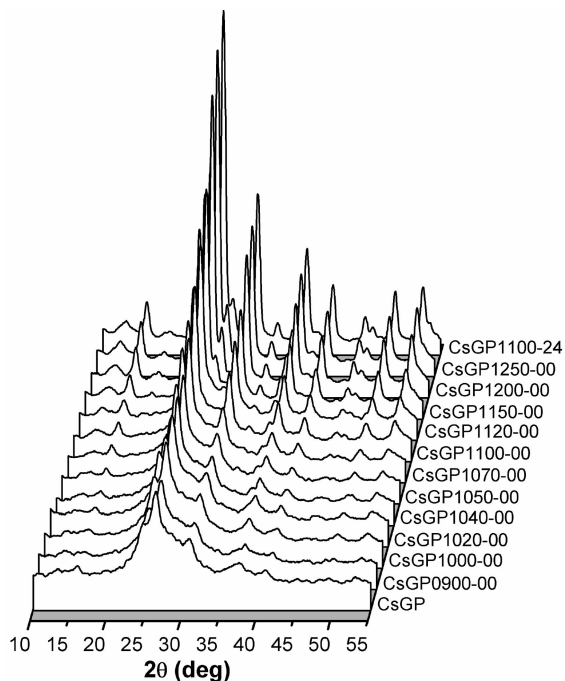


**Figure 2.** X-ray diffractogram of Cs-geopolymer heated to various temperatures. Samples are labeled according to Table 1. Data was collected using a laboratory-based Rigaku (D-Max II) X-ray powder diffractometer (Rigaku/USA Inc., Danvers, MA) equipped with a Cu K $\alpha$  source ( $\lambda = 0.1540598$  nm), and a single crystal monochromator in the diffracted beam path was used to acquire XRD patterns in Bragg–Brentano geometry over a  $2\theta$  range of  $5\text{--}75^\circ$  with a step size of  $0.02^\circ$ .

(above  $1000^\circ\text{C}$ ) showed development of crystalline pollucite phase. The average elemental composition for CsGP, as determined using EDS analysis, was Al =  $9.3 (\pm 0.7)$  atomic %, Si =  $19.3 (\pm 0.7)$  atomic %, and Cs =  $12.5 (\pm 2.3)$  atomic %, with remainder being accounted for by O as  $58.9 (\pm 1.0)$  atomic % (Note: water was not included in the calculation). Although the average elemental composition remained invariant with temperature for all the samples reported in this study, the large variation in Cs in the CsGP sample is particularly notable. For example, the Cs content varied by approximately 19% when measured at seven different locations in the pressed pellet specimen of the CsGP powder. This reflects in the similar variability in Cs/Si or Cs/Al ratios, which were found to be  $0.64 (\pm 0.12)$  and  $1.34 (\pm 0.27)$ , respectively. The Si/Al ratio, on the other hand, was fairly constant at  $2.08 (\pm 0.18)$ . These findings are consistent with earlier reports on the synthesis of geopolymers with a Si/Al = 2, where metakaolin was not completely dissolved.<sup>14,31,32</sup> As a result, not all of the Cs in solution is bound within the structure and may be distributed nonuniformly throughout the set geopolymer, often migrating to the surface along with pore water. Upon evaporation of water, Cs may be deposited on particle surfaces or on pore walls as CsOH or even in the carbonate form. Therefore, it is quite reasonable that even upon grinding to fine powder, variability in Cs concentration was observed on a local scale.

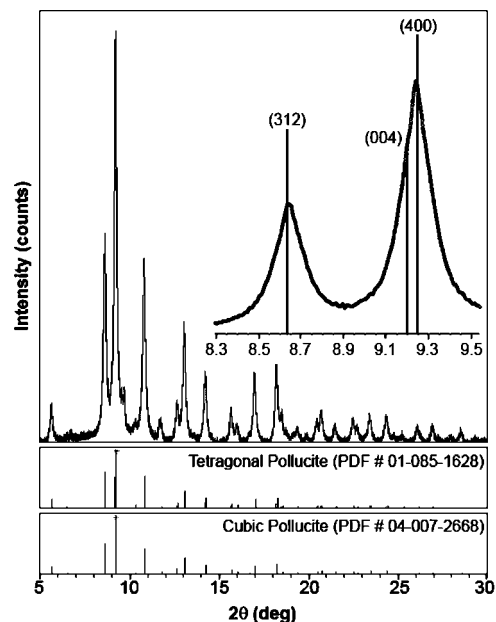


**Figure 3.** Synchrotron X-ray diffractogram of Cs-geopolymer heated to  $1100^\circ\text{C}$  for 24 h, compared with both tetragonal<sup>33</sup> and cubic<sup>34</sup> pollucite models. The inset is an enlarged view of peaks in the  $8.3\text{--}9.5^\circ 2\theta$  range, with the tetragonal model superimposed. The symmetric shape of the peak centered at  $9.25^\circ 2\theta$  confirms that pollucite is in the cubic state. Data was collected at  $22.5$  keV ( $\lambda \approx 0.5515$  Å) between  $0\text{--}37^\circ 2\theta$  in transmission geometry with a step size of  $0.00095^\circ$  in  $2\theta$ .

On the basis of prior studies, pollucite is expected to transform from a cubic to a tetragonal phase, that is, from space group symmetry  $Ia\bar{3}d$  to  $I41/a$ , near room temperature.<sup>33,34</sup> Nonetheless, there is no consensus on the pollucite phase stable at room temperature. Pollucite is topologically equivalent to leucite ( $\text{KAlSi}_2\text{O}_6$ ); however, the transition temperature of pollucite is lower due to the stabilizing effect of a larger  $\text{Cs}^+$  ion on the aluminosilicate framework.<sup>20</sup> Although no phase transitions were observed in the DSC/TGA studies when the sample was cooled from  $1300^\circ\text{C}$  to room temperature (Figure 1), more careful examination using XRD was deemed essential. A unit cell of pollucite consists of a network of 48 corner-shared Si–O or Al–O tetrahedra with 16  $\text{Cs}^+$  ions located in cavities, 12-coordinated with respect to oxygen.<sup>35,36</sup> Large cavities are formed as the tetrahedra are linked to form 4-, 6-, and 8-membered rings. The 8-membered rings create elongated cages which permit large cations such as  $\text{Cs}^+$  and  $\text{Rb}^+$  to pass through 6-membered rings. In the tetragonal phase, the 8-membered rings are further elongated, causing a crumpling of the 4-membered rings.<sup>19</sup> To determine the symmetry of the pollucite phase formed by crystallization of CsGP, high resolution synchrotron XRD patterns were collected for the CsGP1100–24 sample (Figure 3). On the basis of the observed peaks, it was concluded that, upon heating, the CsGP transformed into cubic pollucite phase and remained cubic after cooling to room temperature.

(31) Duxson, P.; Provis, J. L.; Lukey, G. C.; Separovic, F.; van Deventer, J. S. J. *Langmuir* **2005**, *21*, 3028.

(32) Kriven, W. M.; Bell, J.; Gordon, M. Microstructure and Microchemistry of Fully-Reacted Geopolymers and Geopolymer Matrix Composites. *Ceramic Transactions*; American Ceramic Society: Westerville, OH, 2003; p 227 (105th Annual Meeting of the American Ceramic Society, Nashville, TN, 2003).

(33) Palmer, D. C.; Dove, M. T.; Ibberson, R. M.; Powell, A. M. *Am. Mineral.* **1997**, *82*, 16.

(34) Yanase, I.; Kobayashi, H.; Shibasaki, Y.; Mitamura, T. *J. Am. Ceram. Soc.* **1997**, *80*, 2693.

(35) Náray-Szabó, S. Z. *Kristallogr.* **1938**, *99*, 277.

(36) Taylor, W. H. Z. *Kristallogr.* **1938**, *99*, 283.

**Table 2. Refinement Results for Geopolymer Sample Heated to 1100 °C for 24 h**

refinement <i>r</i> -range (Å)	<i>R<sub>w</sub></i>	lattice parameter (Å)	isotropic temperature factors ⟨ <i>u</i> <sup>2</sup> ⟩	scale factor
10.0–30.0	11.19 <sup>a</sup>	13.6573(15)	Cs = 0.03254(13) Si = 0.0115(3) Al = 0.065(3) O = 0.0584(7)	0.423(6)
1.0–30.0	19.00 <sup>b</sup>	13.6608(21)	Cs = 0.04631(20) Si = 0.0353(3) Al = 0.0224(3) O = 0.06644(33)	0.446(3)
1.0–10.0	21.28 <sup>b</sup>	13.663(6)	Cs = 0.0472(3) Si = 0.0347(3) Al = 0.0231(4) O = 0.06679(25)	0.442(4)

<sup>a</sup> Refinement initialized using structural data from Yanase et al.<sup>34</sup>

<sup>b</sup> Refinement initialized using structural data from the 10.0–30.0 Å refinement. The parameters included in the refinement were the lattice parameters, scale factors, correlation factor linear, low *r* peak sharpening, *Q*-sigma (peak dampening), and isotropic temperature factors.

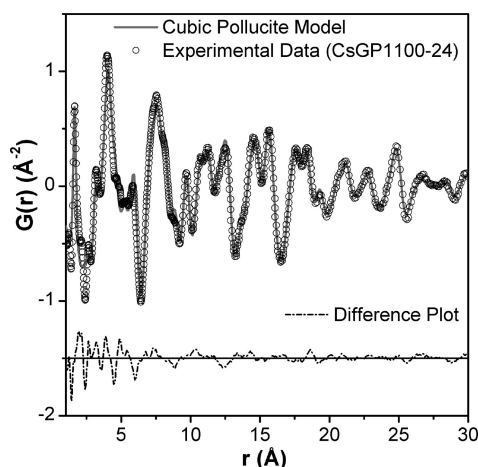


**Figure 4.** Refinement results for Cs geopolymer heated to 1100 °C for 24 h (circles) compared to the cubic pollucite model (line), with a difference plot shown below.

**Structure Refinement of Crystallized Cs-Geopolymer.** The transition to crystalline phase observed in Cs-geopolymer suggests a probable relationship between the pollucite and Cs-geopolymer structures. Total scattering methods can provide invaluable insight when studying amorphous materials or materials with considerable intrinsic disorder and short coherence lengths.<sup>37,38</sup> Both the short- and the long-range order in crystallized Cs-geopolymer was examined by using the PDF method. The atomic PDF of the crystallized Cs-geopolymer powder sample, which had been heated to 1100 °C for 24 h (sample CsGP1100-24), was compared with a cubic pollucite structure<sup>34</sup> using the program PDFFIT 1.0.3. The theoretical PDF pattern for cubic pollucite phase was refined to obtain the best fit to experimental data collected for the crystallized Cs-geopolymer. Following refinement, the partial contribution of each atom–atom pair was calculated to determine how specific pair correlations contributed toward the overall PDF. The results of these refinements are shown in Table 2 and Figure 4.

For the crystallized Cs-geopolymer sample (CsGP1100-24), the best fit was obtained over the refinement range from

10–30 Å, with a poorer fit over the 1–10 Å range. A plot of the difference between the refined model and experimental data illustrates this behavior (Figure 4). Because of this, the results of the 10–30 Å refinement were used as a starting point for the 1–30 Å and 1–10 Å refinements. As shown in Table 2, the goodness of fit is determined using a weighted *R* value, *R<sub>w</sub>*, calculated according to eq 4:

$$R_w = \sqrt{\frac{\sum_{i=1}^N w(r_i) [G_{\text{obs}}(r_i) - G_{\text{calc}}(r_i)]^2}{\sum_{i=1}^N w(r_i) G_{\text{obs}}^2(r_i)}} \quad (4)$$

Here, *G<sub>obs</sub>* is the experimental PDF, *G<sub>calc</sub>* is the calculated PDF, *N* is the number of data points, and *w(r<sub>i</sub>)* is the weight associated with each datum.

Regardless of the refinement range, the lattice parameters calculated for the cubic pollucite phase were smaller than those reported by Yanase et al.<sup>34</sup> In addition, the isotropic temperature factor for oxygen was higher than that of the model (0.0215) and is indicative of increased disorder. Minor improvement in the fitting of the low-*r* region was possible when correlated thermal motion was taken into consideration, particularly in the range up to *r* = 3.25 Å. Nearest neighbor T–O bonds, where T represents tetrahedral Si or Al, are strong and are well-known to exhibit correlated thermal motion<sup>39,40</sup> which causes a sharpening of the initial T–O peak.<sup>41</sup> It should be noted that Si and Al in tetrahedral configuration are fairly indistinguishable from each other in X-ray PDF analysis due to their very similar X-ray scattering cross sections.<sup>8</sup>

The crystallized Cs-geopolymer and cubic pollucite models correlate well at high *r*. The poorer fit at low *r* is most likely due to factors such as correlated thermal motion of atoms which can cause sharpening of the low *r* peaks and/or termination errors which may result in appearance of spurious extra peaks. Besides the above two factors, it is believed that the poorer fit at low *r* could also be due to the presence of a secondary amorphous phase. As was discussed earlier, incompletely dissolved metakaolin and extrastructural Cs in the pore water can be present in geopolymers with Si/Al = 2. It is expected that upon heating the water will evaporate, and the CsOH which is left behind will subsequently react to form Cs silicates or Cs aluminosilicates at higher temperatures.<sup>42</sup> Any remnant metakaolin either should convert to mullite (3Al<sub>2</sub>O<sub>3</sub>·2SiO<sub>2</sub> or Al<sub>6</sub>Si<sub>2</sub>O<sub>13</sub>) and silica (SiO<sub>2</sub>) when heated to 1100 °C for 24 h or may react with CsOH to form Cs aluminosilicates.<sup>42,43</sup> Given the good fit of the

- (37) Gateshki, M.; Niederberger, M.; Deshpande, A. S.; Ren, Y.; Petkov, V. *J. Phys.: Condens. Matter* **2007**, *19*, 156205.
- (38) Gateshki, M.; Petkov, V.; Hyeon, T.; Joo, J.; Niederberger, M.; Ren, Y. *Solid State Commun.* **2006**, *138*, 279.
- (39) Bartelmehs, K. L.; Downs, R. T.; Gibbs, G. V.; Boisen, M. B.; Birch, J. B. *Am. Mineral.* **1995**, *80*, 680.
- (40) Downs, R. T.; Gibbs, G. V.; Boisen, M. B. *Am. Mineral.* **1990**, *75*, 1253.
- (41) Jeong, I. K.; Heffner, R. H.; Graf, M. J.; Billinge, S. J. L. *Phys. Rev. B* **2003**, *67*, 104301.
- (42) Bailar, J. C. *Comprehensive Inorganic Chemistry*; Pergamon Press: Elmsford, NY, 1973.
- (43) Chen, Y. F.; Wang, M. C.; Hon, M. H. *J. Eur. Ceram. Soc.* **2004**, *24*, 2389.

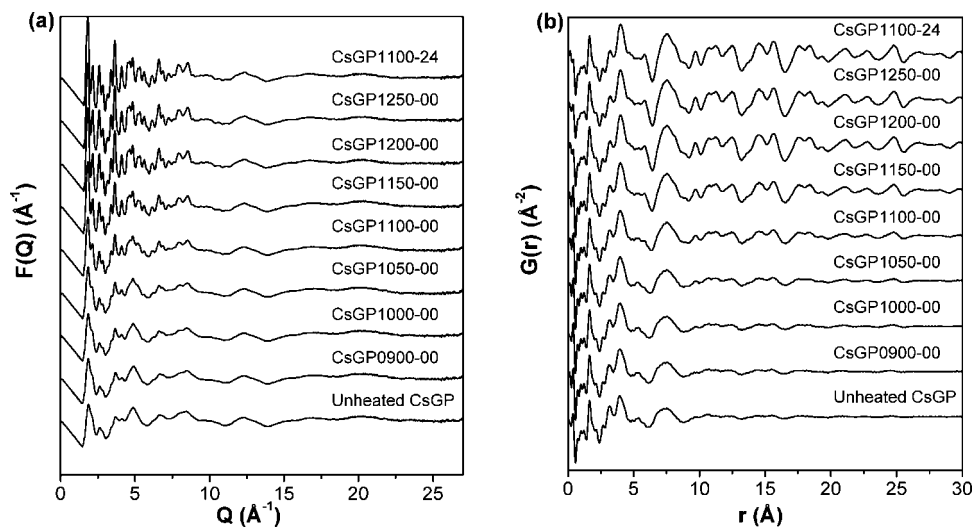


**Figure 5.** (a) Reduced structure functions for Cs geopolymer heated to various temperatures and (b) the resultant PDFs after Fourier transformation. Successive plots are vertically offset and labeled according to Table 1.

model to the data at high  $r$ , it is unlikely that mullite crystallized on heating. The poorer fit at low  $r$  is better explained by formation of glassy Cs-silicate or Cs-aluminosilicate phases or a combination of the two phases.<sup>42</sup> Given that these glassy phases lack long-range order, they would contribute only toward the low  $r$  portion of the data.

**PDF Analysis of Cs-Geopolymer.** The PDF method provides the first direct measurement of the length scale of the structural ordering in unheated geopolymers. The CsGP has an ordered structure up to  $\sim 9$   $\text{\AA}$  which resembled that of the crystalline pollucite. The reduced structure-function  $F(Q)$  and the corresponding PDF plots for Cs-geopolymers heat treated to different temperatures are shown in Figure 5.  $F(Q)$  for the unheated geopolymer showed broad peaks, which is characteristic of amorphous materials. The  $F(Q)$  patterns were fairly similar for samples heated to  $\leq 1000$   $^{\circ}\text{C}$ , but at temperatures  $\geq 1050$   $^{\circ}\text{C}$  the peaks in the low- $Q$  region developed finer structure and several narrower peaks, which is indicative of development of long-range ordering. All samples showed matching broad oscillations beyond  $10$   $\text{\AA}^{-1}$  in  $F(Q)$ , which reaffirms the similarity in their local bonding environment. The CsGP and samples heated to  $\leq 1000$   $^{\circ}\text{C}$  have very similar PDFs as well (Figure 5b).

Cubic pollucite has a unit cell with a lattice parameter of  $13.66$   $\text{\AA}$ ,<sup>34</sup> and the CsGP has notable ordering below this length scale, which gives rise to broad peaks in laboratory-based X-ray analysis. The order seen in CsGP is similar to that found in glasses and other noncrystalline materials<sup>8,44,45</sup> and is consistent with the widely accepted X-ray amorphousness of these materials. An earlier  $^{29}\text{Si}$  MAS NMR investigation<sup>31</sup> showed that framework ordering was present to the nearest-tetrahedral-neighbor length scale ( $\sim 3$   $\text{\AA}$ ), and a statistical thermodynamic model also suggested that some order could extend to the next-nearest-tetrahedral sites ( $\sim 5$ – $6$   $\text{\AA}$ ).<sup>15</sup> However, these studies were limited to description of the ordering of the tetrahedral cations within the framework and

not the framework topology, extra-framework cations, or oxygen sites.

The PDFs are overlaid in Figure 6, and they illustrate how long-range order systematically increased as a function of temperature between  $900$  and  $1200$   $^{\circ}\text{C}$  due to crystallization of CsGP into pollucite. The partial PDF contributions from various major pair–pair correlations as determined from the cubic pollucite model of Yanase et al. are also shown.<sup>34</sup> For example, the first noticeable peak centered near  $1.66$   $\text{\AA}$  is due to T–O bonds. Si–O bonds are expected to have a range of lengths centered near  $1.60$   $\text{\AA}$  while the length distribution of tetrahedral Al–O is centered at  $1.75$   $\text{\AA}$ .<sup>8</sup> Peaks at  $r$  values lower than the T–O peak are artifacts due to data termination errors (i.e., finite- $Q$ ) or imperfect corrections, and their amplitudes provide a measure of the quality of the PDF data.<sup>46</sup> Most of the peaks present are the result of multiple pairs and, beyond  $3$   $\text{\AA}$ , are dominated by pairs involving Cs, largely due to the high X-ray scattering cross section of cesium.

The T–O peak position (at  $\sim 1.66$   $\text{\AA}$ ) is unchanged with temperature, which indicates that the T–O bond characteristics remain the same even after pollucite crystallization. However, the peak assigned to T–T correlations and centered near  $3.20$   $\text{\AA}$  in the unheated sample sharpened, decreased in amplitude, and became similar to that observed for pollucite as the CsGP sample was heated to  $900$   $^{\circ}\text{C}$ . To definitively determine the cause of this change, PDF data were collected for (a)  $10.1$  M CsOH solution, (b) as-received metakaolin, and (c) metakaolin heated to  $900$   $^{\circ}\text{C}$ . Consistent with the findings of Babu et al.,<sup>47</sup> the hydrated  $\text{Cs}^+$  ions have a Cs ion–water pair correlation peak near  $3.2$   $\text{\AA}$ , which coincides with the T–T peak location of pollucite as shown in Figure 7. Metakaolin also has a T–T peak in this region (see Figure 7) but showed no change upon heating to  $900$   $^{\circ}\text{C}$ . There is also a remote possibility that rearrangement of the Al and Si tetrahedra in the geopolymer network may result in the observed decrease in amplitude for T–T correlations.

(44) Petkov, V.; Gerber, T.; Himmel, B. *Phys. Rev. B* **1998**, *58*, 11982.

(45) Petkov, V.; Ohta, T.; Hou, Y.; Ren, Y. *J. Phys. Chem. C* **2007**, *111*, 714.

(46) Toby, B. H.; Egami, T. *Acta Crystallogr., Sect. A* **1992**, *48*, 336.

(47) Babu, C. S.; Lim, C. *J. Phys. Chem. B* **1999**, *103*, 7958.



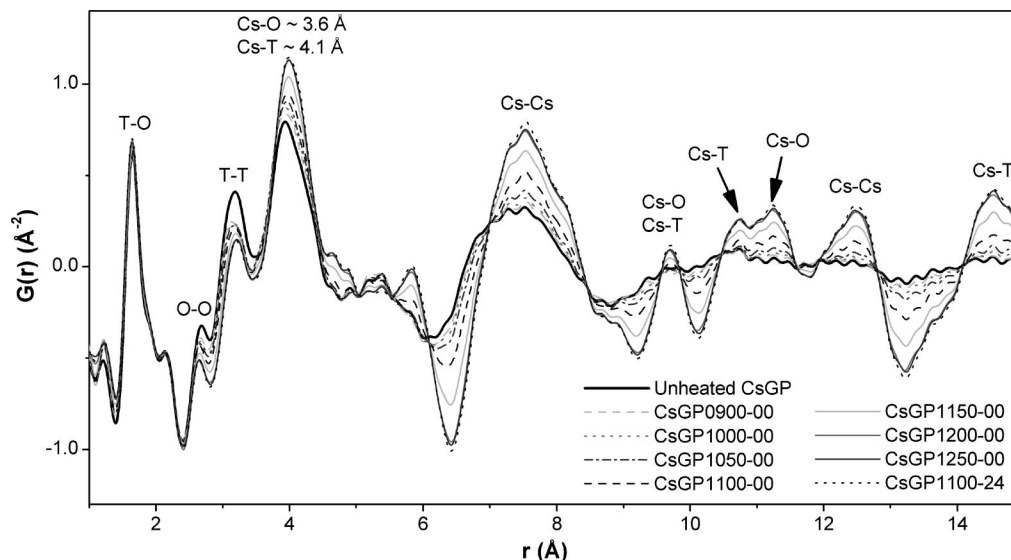


**Figure 6.** Experimental PDFs for Cs geopolymer with successive plots overlaid. The major partial contributions are labeled according to the calculated PDF for cubic pollucite using the refined parameters from Yanase et al.<sup>34</sup>

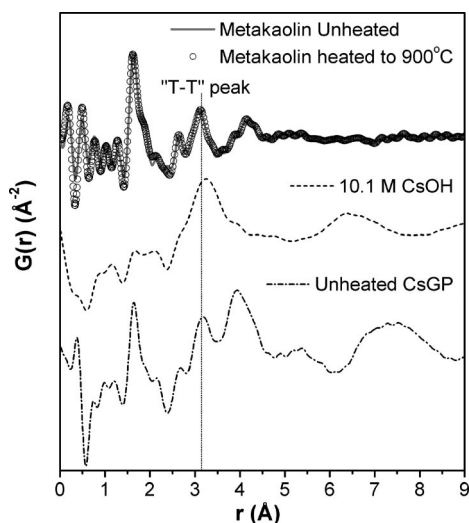


**Figure 7.** Experimental PDFs for unheated Cs geopolymer (bottom), 10.1 M CsOH solution (middle), and an overlay of unheated metakaolin (line) and metakaolin heated to 900 °C (circles) (top).

However, this is unlikely in the absence of any other structural changes in the PDF between the unheated samples and samples heated up to 900 °C.

Therefore, the evolution of the T–T peak centered near 3.20 Å between CsGP and CsGP900-00 was due to the presence of hydrated cesium, which was dehydroxylated by 900 °C. This is consistent with thermogravimetric analysis of CsGP in Figure 1, which showed that most of the water was removed by 900 °C. This finding supports a structural model proposed by Barbosa et al. for Na-geopolymer,<sup>48</sup> in which hydrated Na<sup>+</sup> cations are located within the aluminosilicate matrix and balance the negative charge on the AlO<sub>4</sub><sup>−</sup> tetrahedra. Cesium ion–water correlations could be due to hydrated cesium within the geopolymer tetrahedral cavities or in void spaces in the structure. Pore water expelled from the geopolymer after setting was highly alkaline, and

was found to contain primarily Cs<sup>+</sup> and a very small amount of dissolved silica.

**Insights into the Geopolymer Structure.** The remarkable similarities observed in short to medium range order between CsGP and pollucite suggest that only minor atomic rearrangements in CsGP structure should be required to transform it into crystalline pollucite. Despite these similarities, there are a few notable differences between the pollucite structure and that of unheated geopolymer. Figure 8 shows PDF plots of the optimum refined cubic pollucite model and the unheated geopolymer over  $r = 1\text{--}10$  Å along with the contribution of various partial PDFs. The evolution observed in the T–T peak (near 3.2 Å) upon heating the Cs-geopolymer was discussed earlier, and dehydration of the cesium ion was identified as the most probable reason. As water is expelled from the geopolymer structure, the Cs ion–water correlation (peak at 3.2 Å) decreases while a more prevalent Cs–T correlation is formed (the large peak centered just below 4 Å). As a consequence, the peak observed in the Cs-geopolymer appears to shift toward a higher  $r$ . The increase in Cs–T correlations is due to the association of Cs with negatively charged oxygen sites in the aluminosilicate framework and results in transformation of the Cs-geopolymer structure into pollucite.

Prior to this study, it was not known whether Cs<sup>+</sup> cations would be hydrated within a geopolymer structure. The uncertainty was primarily because (a) Cs<sup>+</sup> cations are expected to hydrate much less strongly than do Na<sup>+</sup> or K<sup>+</sup>,<sup>47</sup> and (b) a hydrated Cs<sup>+</sup> complex may be too large to fit within the aluminosilicate framework structure of pollucite. In the case of geopolymers, it is possible that the aluminosilicate network, which is comprised of corner-shared tetrahedra of Al and Si, is formed around the hydrated Cs<sup>+</sup> cation. The structure of unheated geopolymer is disordered, unlike crystalline pollucite. The lack of long-range order in geopolymers is possibly due to kinetic constraints imposed by the rapid and low temperature setting of geopolymers. However, expulsion of water from geopolymer structure enables

(48) Barbosa, V. F. F.; MacKenzie, K. J. D.; Thaumaturgo, C. *Int. J. Inorg. Mater.* **2000**, 2, 309.

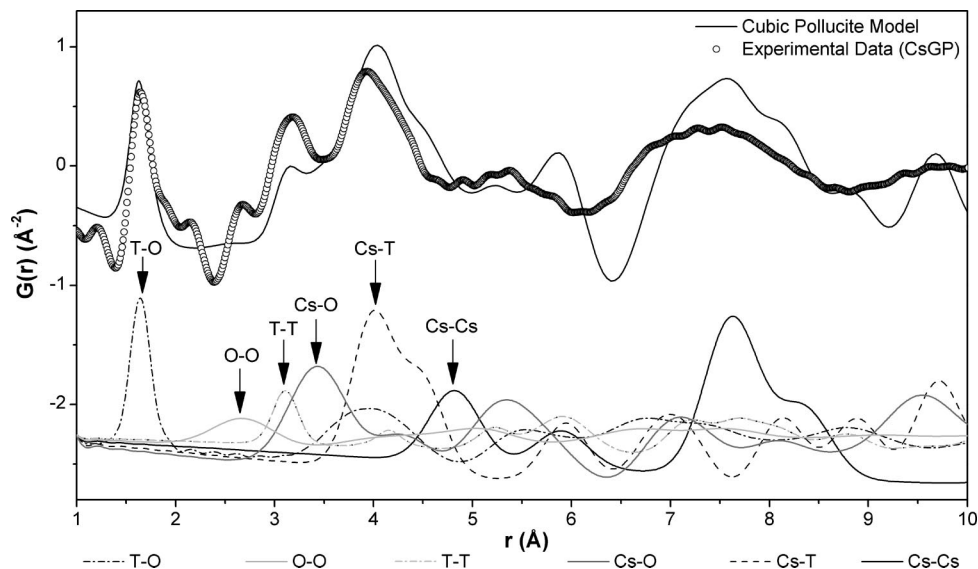


**Figure 8.** PDFs of unheated CsGP (circles) compared to cubic pollucite model (line) refined with respect to the CsGP1100-24 heated geopolymer sample in the range 1–10 Å. The partial PDF contributions computed from the refined model are included below (legend shown below plot).

rearrangement of the Si/Al tetrahedral network to form the pollucite structure. The PDF of the unheated geopolymer resembles, but does not precisely match, that of the pollucite model in Figure 8 near  $r = 4.75$  Å where the first Cs–Cs partial is located. If this first Cs–Cs correlation was absent in the geopolymer at 4.75 Å, the PDF would be negative in this region. It is therefore reasonable to suggest that the  $\text{Cs}^+$  location in the as-synthesized geopolymer is not dissimilar to that in pollucite, with minor differences due to the hydration of the cesium cation and the somewhat disordered structure of the geopolymer compared to crystalline pollucite.

Another notable observation was that except for the T–T correlation peak, little change was observed in the short-range order in the PDF patterns upon heating to 1000 °C. Since nearly all of the water was lost by 900 °C, it is suggested that most of the water present in CsGP was not associated with Al–OH or Si–OH bonds. In PDF studies involving noncrystalline materials, the low  $r$  peaks can be broadened compared to the bulk crystalline phase due to a more disordered or strained environment.<sup>37</sup> For example, in mullite synthesis via sol–gel processing, the initial T–O peak is broadened in unheated gels due to Al–OH, Si–OH, and Si–OR (R: residual organic) groups.<sup>49</sup> Upon heating, the peak sharpens and shifts toward lower  $r$  as Si–O–Si, Si–O–Al, and Al–O–Al bonding angles decrease. The remarkable stability of the T–O peak with temperature in geopolymers suggests that the (Si,Al)–O bonding environment in the geopolymer is nearly identical to that in the final crystalline pollucite, and the water present is most likely contained within nanopores in the microstructure or along with the hydrated  $\text{Cs}^+$  cation.

### Conclusions

For the first time a quantitative view of the atomistic ordering in Cs-based geopolymer has been revealed. The

short-range structure of as-synthesized geopolymer has considerable resemblance to that of cubic pollucite up to a length scale of  $\sim 9$  Å. Hydrated  $\text{Cs}^+$  ions are present in the Cs-geopolymer structure and are not strictly associated with the network oxygen sites as is the case for pollucite. These findings provide support for previously proposed models which suggested that hydrated alkali cations are present in cavities within the geopolymer gel structure.

The PDF of crystalline pollucite formed from heated geopolymer agreed very well with a cubic pollucite model above 10 Å but had a poorer fit at low  $r$ . PDF correlations involving Cs systematically grew in intensity between 1000–1200 °C as  $\text{Cs}^+$  ions moved into crystallographically favorable positions and long-range order, resembling cubic pollucite, developed.

This study has clearly demonstrated the potential of total scattering methods in understanding complex material systems such as geopolymers. The transformation from short- to long-range order, that is, from geopolymer to a crystalline ceramic phase, was successfully utilized to elucidate the geopolymer structure. This study provides the basis for further investigations in geopolymeric systems using the PDF method to understand the role of different factors such as the type of alkali cations, Si/Al ratio, and so forth, in the geopolymer structure.

**Acknowledgment.** This work was supported by Air Force Office of Scientific Research (AFOSR), USAF, under Nanoinitiative grant No. FA9550-06-1-0221. Dr. Pankaj Sarin and Ryan P. Haggerty were supported by an AFOSR grant No. FA9550-06-1-0386. Dr. John L. Provis was supported by a one year Australian-American Fulbright Postgraduate Scholarship and a University of Melbourne Postgraduate Overseas Research Experience, as well as through the Particulate Fluids Processing Centre (a special Research Centre of the Australian Research Council). Experimental work was conducted at the Advanced Photon Source, Argonne National Laboratory, which is supported by the U.S. Department of Energy, Office of Science, and Office of Basic Energy Sciences, under Contract No. DE-AC02-06CH11357. The authors also ac-

(49) Okuno, M.; Shimada, Y.; Schmucker, M.; Schneider, H.; Hoffbauer, W.; Jansen, M. *J. Non-Cryst. Solids* **1997**, *210*, 41.



knowledge the use of facilities at the Center for Microanalysis of Materials, Frederick Seitz Research Laboratory (at the University of Illinois at Urbana–Champaign), which is partially supported by the U.S. Department of Energy under grant No. DEFG02-91-ER45439. The authors would like to thank Prof. Valeri Petkov (Central Michigan University) for

useful discussions and running preliminary samples and Dr. Karena Chapman (Advanced Photon Source, Argonne National Laboratory) for her help with the PDFgetX2 program.

CM703369S